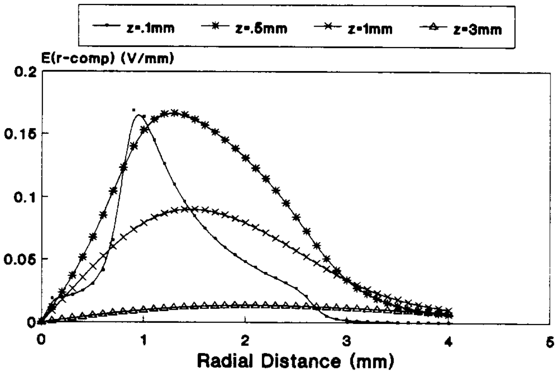

Fig. 5. Radial electrical field intensity versus distance on various planes perpendicular to coaxial axis. (a = 0.824 mm, b = 2.655 mm.)

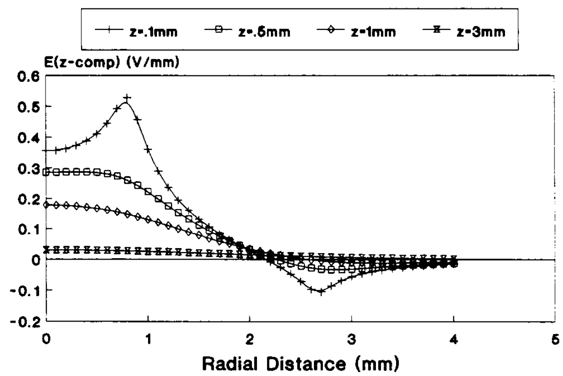

Fig. 6. Axial electrical field intensity versus distance on various planes perpendicular to coaxial axis. (a = 0.824 mm, b = 2.655 mm.)

a peak value near ρ = 0.8 mm (which corresponds to the radius of the inner conductor, a = 0.0824 cm) and falls off as radial distance increases, closely following the inverse relation with the radial distance for a TEM field ($E_\rho \propto 1/\rho$). A distinct change in the characteristic is to be noted around ρ = 2.6 mm, which corresponds to the radius of the outer conductor of the coaxial line (b = 0.2655 cm). As the observation plane moves away from the aperture, the field magnitudes decrease in both figures; and for z = 3.0 mm, the magnitudes of both components of electric field intensity drop to a relatively small value.

IV. Conclusion

A spectral domain approach has been used to analyze the aperture fields of an open-ended coaxial line terminated in a two-layered dielectric medium. The aperture capacitance as a function of dielectric layer thickness has been calculated for three different dielectrics backed by metal or air and compared with the available data. The electric field intensity near the aperture has been determined and used to explain the physics of the problem. Theoretically, the layer thickness d should be large in comparison with the outer conductor radius b of the line in order to simulate an infinitely thick dielectric medium. However, the results indicate that the errors are small even for $d \sim b$.

It is to be noted that the results reported in this paper are expected to be fairly accurate at low frequencies with no radiation fields. A full-wave analysis is needed to account for radiation fields as well as the discrete guided wave modes that the layered system can support [10].

References

[1] M. A. Stuchly and S. S. Stuchly, "Coaxial line reflection method for measuring dielectric properties of biological substances at radio and microwave frequencies—A review," *IEEE Trans. Instrum. Meas.*, vol. IM-29, pp. 176–183, Sept. 1980.

[2] E. C. Burdette, F. L. Cain, and J. Seals, "In vivo probe measurement technique for determining dielectric properties at VHF through microwave frequencies," *IEEE Trans. Microwave Theory Tech.*, vol. MTT-28, pp. 414–427, Apr. 1980.

[3] J. R. Mosig, J. C. E. Besson, M. Gex-Fabry, and F. E. Gardiol, "Reflection of an open-ended coaxial line and application to nondestructive measurement of materials," *IEEE Trans. Instrum. Meas.*, vol. IM-30, pp. 46–51, Mar. 1981.

[4] L. S. Anderson, G. B. Gajda, and S. S. Stuchly, "Analysis of an open-ended coaxial line sensor in layered dielectrics," *IEEE Trans. Instrum. Meas.*, vol. IM-35, pp. 13–18, Mar. 1986.

[5] H. Levine and C. H. Papas, "Theory of the circular diffraction antenna," *J. Appl. Phys.*, vol. 22, no. 1, pp. 29–43, Jan. 1951.

[6] J. Galejs, *Antennas in Inhomogeneous Media*. Oxford, U.K.: Pergamon, 1969.

[7] D. K. Misra, "A quasi-static analysis of open-ended coaxial lines," *IEEE Trans. Microwave Theory Tech.*, vol. MTT-35, pp. 925–928, Oct. 1987.

[8] T. W. Athey, M. A. Stuchly, and S. S. Stuchly, "Measurement of radio frequency permittivity of biological tissues with an open-ended coaxial line: Part I," *IEEE Trans. Microwave Theory Tech.*, vol. MTT-30, pp. 82-86, Jan. 1982.

[9] L. L. Tsai, "A numerical solution for the near and far field of an annular ring of magnetic current," *IEEE Trans. Antennas Propag.*, vol. AP-20, pp. 569-576, Sept. 1972.

[10] R. Chatterjee, *Advanced Microwave Engineering*. Chichester, U.K.: Ellis Horwood, 1988.

Dielectric Characterization of Printed Circuit Board Substrates

C. HEYWARD RIEDELL, MICHAEL B. STEER, MEMBER, IEEE, MIKE R. KAY, JEFFEREY S. KASTEN, MEMBER, IEEE, MARK S. BASEL, MEMBER, IEEE, AND REAL POMERLEAU

Abstract—**The design and quality assurance of high-speed digital systems requires a fast and accurate method for the electrical characterization of printed circuit substrates. This paper presents a new technique for measuring the dielectric properties of such substrates based on the measured scattering parameters of a transmission line. The method is broad band, determines the effective permittivity and loss tangent, and is compatible with existing substrate quality assurance schemes. Comparisons with alternative permittivity characterization techniques are presented.**

I. Introduction

The design of high clocking speed digital systems requires accurate characterization of printed circuit board (PCB) substrates. As clock frequencies continue to increase, circuit designers must be more aware of transmission impairments caused by impedance mismatch, coupling, and transmission line discontinuities. Improved material characterization leads to more accurate circuit sim-

Manuscript received May 15, 1989.

C. H. Riedell, M. R. Kay, and R. Pomerleau are with BNR, Research Triangle Park, NC 27709.

M. B. Steer, J. S. Kasten, and M. S. Basel are with the Center for Communications and Signal Processing, Department of Electrical and Computer Engineering, North Carolina State University, Raleigh, NC 27695.

IEEE Log Number 8933414.

ulation during the design phase and tighter control of signal performance after board fabrication.

PCB materials are anisotropic and nonhomogeneous which complicates permittivity characterization. Thus the electromagnetic field orientation of fabricated planar transmission lines must be preserved in any dielectric characterization test structure. The preservation of field orientation is more critical with proposed multilayer high-speed composites of such exotic materials as cyanate ester, Teflon, and the traditional fiberglass reinforced resin. These multilayer structures provide a tradeoff of the low dielectric constant but high cost of the exotic materials, and the mechanical rigidity, low water absorption and low cost of the fiberglass materials. An additional consideration in the development of a dielectric test procedure is that it should be compatible with current fabrication practice. Existing PCB fabrication processes yield a test coupon (typically 1 by 10 in) for mechanical testing. This coupon could be utilized for substrate characterization of, for example, novel composites or for quality assurance of a standard process.

Current substrate characterization techniques generally measure both the real and imaginary parts of the complex permittivity. Those suited to laminated materials, as used in PCB's, can be divided into four major categories; resonance, reflection/transmission, time-domain reflectometry (TDR), and phase/length comparison.

Resonant method calculations of the complex permittivity are based upon the measurement of the resonant frequency and the quality factor of a resonant circuit of some particular geometry. These methods provide information at only a few discrete, harmonically related frequencies specific to the structures involved [1]–[5]. Of the various resonant structures reported, only the strip resonators, Fig. 1, have the same field distribution as planar circuits.

Reflection/transmission methods are broad band and are based upon measured reflection and transmission coefficients [6], [7]. Consequently, reflection/transmission methods require fewer test structures to obtain information comparable to that obtained from resonant methods. The drawbacks to these methods are the required machining of a dielectric sample and the improper field orientation of the test structure, e.g., see Fig. 2.

TDR methods compare the signal reflected from a test device to the incident signal [8]. Fourier analysis is performed converting the time-domain response into the frequency-domain representation. The complex permittivity can be related to the frequency-domain reflection coefficient and is found numerically. However, the inherent assumption of TDR methods is that the transmission coefficient is unity and so it is not possible to completely remove the effect of test fixturing.

The phase/length comparison method compares the electrical and physical length of a pair of transmission lines [9]. The real part of the permittivity is related to the difference in the electrical lengths divided by the difference in the physical lengths. The main drawback, when compared to the methods previously mentioned, is the inability to determine the imaginary part of the complex permittivity, and hence, the loss tangent.

Our new method, called parameter transformation, utilizes the S parameters of a transmission line measured with an automatic network analyzer (ANA). This measurement is de-embedded to remove connector and adaptor errors. The complex permittivity is then calculated by transforming the error corrected S parameters into impedance parameters and relating them to the transmission line propagation constant. The parameter transformation method is broad band and the field orientation is the same as that occurring in an actual PCB layout. In the body of the paper this new method is developed and comparisons are made with alternative dielectric characterization techniques.

II. Development of Method

The telegraphist's equation of a uniform transmission line [10]:

$$Z_{in} = \frac{Z_L + Z_c \tanh(\gamma L)}{Z_C + Z_L \tanh(\gamma L)} Z_c \tag{1}$$

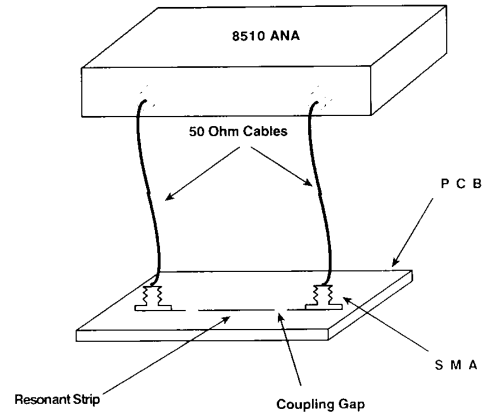

Fig. 1. Test setup for the strip resonator method.

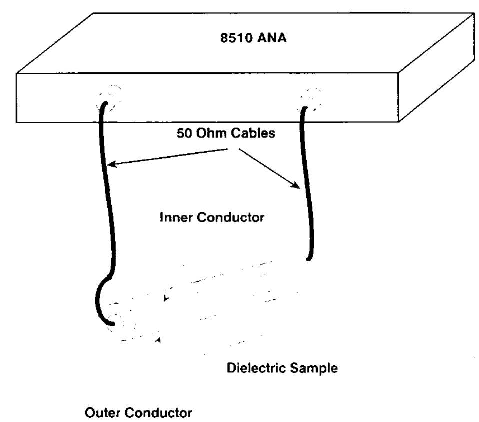

Fig. 2. Test setup for the coaxial reflection method.

relates the input impedance, Z_{in}, of a line to the load impedance, Z_L, at the end of a line to the length, l, propagation constant, γ, and the line's characterisitc impedance, Z_c. From (1) we can derive the z parameters of the line by placing an open circuit and then a short circuit at the end of the line.

If an open circuit is placed at port two, I_2 is zero and the Z_{11} element is equal to the input impedance of the transmission line. Thus the impedance looking into a transmission line with an open circuit at the load is given by

$$Z_{11} = \frac{Z_c}{\tanh(\gamma l)} \tag{2}$$

and the transimpedance by

$$Z_{12} = Z_{21} = Z_c \operatorname{csch}(\gamma l). \tag{3}$$

Transforming these to S parameters [11] and rearranging leads to

$$\gamma = \frac{1}{L} 2 \left(\ln \sqrt{A + A^2 - 1}\right) \tag{4}$$

where

$$A = \frac{(1 + S_{11})^2 + S_{21}^2}{2S_{21}}. \tag{5}$$

Alternatively γ can be found as a byproduct of the TRL de-embedding algorithm [12]. The effective dielectric constant and loss tangent of a nonmagnetic material is related to the propagation constant by

$$\epsilon = \epsilon_0 \epsilon_r = \epsilon_0(\epsilon_r' - j\epsilon_r'') = -\frac{\gamma^2}{\omega^2 \mu_0} \tag{6}$$

and

$$\tan \delta = \frac{\epsilon_r''}{\epsilon_r'}. \tag{7}$$

III. Results

The equipment setup for the parameter transformation method is shown in Fig. 3. A Hewlett Packard 8510 ANA was used to measure the two port S parameters of a planar transmission line fabricated on a stripline PCB. A semi-rigid coaxial cable with a characteristic impedance of 50 Ω connected the ANA to two surface mounted SMA-to-microstrip connectors. These connectors were in turn soldered to the PCB. The S parameters provided by the ANA contain adaptor errors introduced by the connection between the coaxial cables and the actual PCB transmission line. These errors were de-embedded to produce an S parameter description of only the two port transmission line. At this point the data were processed into the dielectric constant and loss tangent, utilizing the impedance parameter transformation and its relationship to the propagation constant.

The parameter transformation technique was compared with the two previously published methods of strip resonance [1]–[5] and coaxial reflection [6], [7]. Measurements for each method were performed on a resin material reinforced with fiberglass (FR4). Figs. 4 and 5 illustrate the dielectric constant and loss tangent calculated for the three techniques. The resonant technique produces discrete results and is plotted as such. The other two methods are broad-band techniques and are plotted as continuous functions of frequency.

IV. Discussion

The results in Figs. 4 and 5 indicate that all three methods compare favorably in the calculation of a dielectric constant of about 4.3. Both the parameter transformation method and the coaxial reflection technique have a slightly lower calculation of the loss tangent (0.02–0.03) than does the resonant method (0.04). This difference is to be expected for the coaxial technique, since it only provides accurate information for loss tangents with values greater than 0.1 [6]. The accuracy of the parameter transformation method is affected by the numerical precision of the measured data. Application of this technique to several S parameter data sets generated with a microwave simulator showed reduced performance in regions where the magnitude of S_{11} approached a minimum. In addition, some measured data sets produced results with considerable jitter about an average value that followed the trend of the curves in Fig. 5. These regions of uncertainty do not impede interpretation of the final results since the dielectric constant and loss tangent are well behaved with frequency for this FR4 test sample.

V. Conclusion

The parameter transformation technique has several advantages over other dielectric characterization methods. The technique is based upon measurements with the same electromagnetic field distributions as a printed circuit trace. This attribute should lead to more accurate values for anisotropic, nonhomogeneous materials such as the composite substrates being explored for high-speed digital signal propagation. Of all the other techniques, only the strip resonator and phase length comparison methods generate the same field patterns. However, both of these require much more space to generate comparable information, and the resonant technique is not broadband. The test structure for the method presented here is simple to fabricate, does not require machining of samples, provides broadband permittivity characterization, and is compatible with existing test coupons. Results of this technique compare favorably with two established techniques—the coaxial reflection and strip resonator methods.

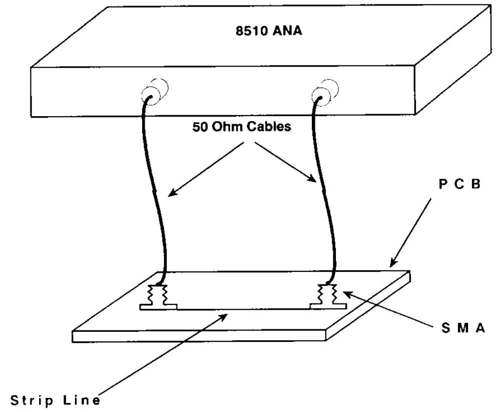

Fig. 3. Test setup for the parameter transformation method.

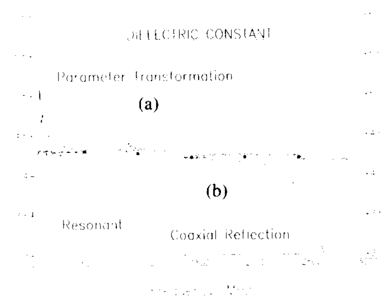

Fig. 4. Real part of the dielectric constant as a function of frequency using (a) the parameter transformation technique developed here and (b) the coaxial reflection method.

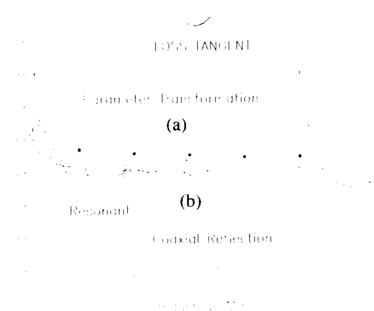

Fig. 5. Loss tangent as a function of frequency using (a) the parameter transformation technique developed here and (b) the coaxial reflection method.

References

[1] M. Olyphant Jr., "Microwave substrates support MIC technology," *Microwaves*, pp. 47–52, Dec. 1980.

[2] M. Olyphant, Jr. and J. H. Ball, "Strip-line methods for dielectric measurements at microwave frequencies," *IEEE Trans. Elect. Insulation*, vol. EI-5, pp. 26–32, March 1970.

[3] T. C. Edwards and R. P. Owens, "2–18-GHz dispersion measurements on 10–100 Ohm microstrip lines on sapphire," *IEEE Trans. Microwave Theory Tech.*, vol. MTT-24, pp. 506–513, Aug. 1976.

[4] S. Deibele and J. B. Beyer, "Measurements of microstrip effective relative permittivities," *IEEE Trans. Microwave Theory Tech.*, vol. MTT-35, pp. 535–538, May 1987.

[5] S. Hubbell and D. J. Angelakos, "A technique for measuring the effective dielectric constant of a microstrip line," *IEEE Trans. Microwave Theory Tech.*, vol. MTT-31, pp. 687–688, Aug. 1983.

[6] S. Tashiro, "Measuring the dielectric constant of solids with the HP 8510 Network analyzer," Product Note 8510-3, Hewlett-Packard Instrumentation Company, Aug. 1985.
[7] W. Barry, "A broad-band, automated, stripline technique for the simultaneous measurement of complex permittivity and permeability," *IEEE Trans. Microwave Theory Tech.*, vol. MTT-34, pp. 80-84, Jan. 1986.
[8] C. Boned and J. Peyrelasse, "Automatic measurement of complex permittivity (from 2 MHz to 8 GHz) using time domain spectroscopy," *J. Phys. E.*, vol. 15, pp. 534-538, May 1982.
[9] N. K. Das, S. M. Voda, and D. M. Pozar, "Two methods for the measurement of substrate dielectric constant," *IEEE Trans. Microwave Theory Tech.*, vol. MTT-35, pp. 636-641, July 1987.
[10] J. D. Kraus, *Electromagnetics.* New York: McGraw-Hill 1984, p. 404.
[11] R. E. Collin, *Foundations for Microwave Engineering.* New York: McGraw-Hill 1966, p. 201.
[12] J. P. Mondal and T-H. Chen, "Propagation constant determination in microwave fixture de-embedding procedure," *IEEE Trans. Microwave Theory Tech.*, vol. 36, pp. 706-714, Apr. 1988.

A Modified Linearized Thermistor Thermometer Using an Analog Multiplier

SUNDARAM NATARAJAN, SENIOR MEMBER, IEEE

Abstract—**Recently, a scheme to measure temperature using a thermistor probe was suggested in [1]. A modification to this scheme is suggested in this paper.**

I. Introduction

A new scheme to measure temperature using a thermistor probe has recently been suggested in [1]. In this circuit, the authors have cleverly used an analog multiplier in the divide mode to eliminate the need to know the actual value of the thermistor constant, β. This scheme also provides a wide linear range as it is evidenced in their experimental results. However, two problems are noted in the circuit. This scheme requires the generation of a reference voltage $E/2$, and the use of a difference amplifier. Furthermore, a difference amplifier requires tightly matched resistors so that the common mode gain can be made as small as possible. A modification is suggested to this circuit in which these two problems can be eliminated. We also find that only one adjustment is needed for calibration in the modified scheme.

II. Modification

A portion of the circuit of [1, Fig. 2(a)], relevant to our discussion, is shown in Fig. 1. The signal to switch S is fed from an astable multivibrator. The voltage, V_C at the node C of the circuit is expected to be $E(R_f/R_T)$. A simple analysis of this circuit leads to the following:

$$V_C = E\frac{\left(1 - \frac{R_3R_5}{R_4R_6}\right) + \frac{R_f}{R_T}\left(1 + \frac{R_3}{R_4}\right)}{\left(1 + \frac{R_1}{R_2}\right)}. \tag{1}$$

Manuscript received June 17, 1989; revised September 8, 1989.
The author is with Department of Electrical Engineering, Tennessee Technological University, Cookeville, TN 38505.
IEEE Log Number 8933412.

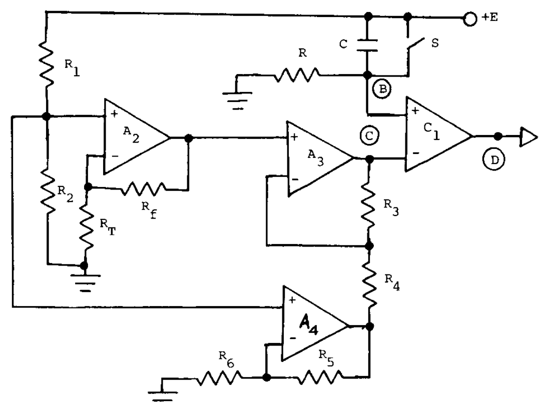

Fig. 1. The relevant portion of the circuit of [1, Fig. 2(a)].

The expected value of $V_C = E(R_f/R_T)$ can only be obtained if the following conditions are satisfied:

$$\frac{R_3R_5}{R_4R_6} = 1 \tag{2a}$$

and

$$\frac{R_1}{R_2} = \frac{R_3}{R_4}. \tag{2b}$$

Otherwise equivalently, one needs to satisfy the following conditions:

$$\frac{R_1}{R_2} = \frac{R_3}{R_4} = \frac{R_6}{R_5}. \tag{3}$$

In practical circuits, even though it is not impossible, it is difficult to achieve the above conditions. One resistor in the difference amplifier must be adjustable so that the common mode gain of the difference amplifier can be made zero. Another variable resistor either R_1 or R_2 is needed to meet the condition of (2b). Furthermore, it is suggested that R_f needs to be adjusted to meet the condition of $R_f = R_{TO}$, where R_{TO} is the resistance of the thermistor at a reference temperature, T_O. This is for calibration purposes. At least three variable resistors are needed in this scheme. These problems can be avoided by using two inverting amplifiers in cascade as shown in Fig. 2. In this circuit, the output voltage V_C is

$$V_C = E\frac{R_f}{R_T}\frac{R_2}{R_1}. \tag{4}$$

Here we need to satisfy $R_2 = R_1$ to obtain a gain of unity (inverting) in the first stage so that $V_C = E(R_f/R_T)$. Indeed the adjustment of $R_2 = R_1$ is not necessary for a reason that will be explained. However, note the simplicity of the circuit of Fig. 2 and the considerable reduction in the number of components. Also note the fact that there is no need to obtain the signal $E/2$ and also no need for any subtraction of signals which can be a considerable problem due to the common mode gain. For calibration purposes, it can be shown that we need to satisfy

$$\frac{R_2R_f}{R_1R_{TO}} = 1 \tag{5}$$

where R_{TO} is the resistance of the thermistor at the reference temperature, T_O. Therefore, the value of R_2 need not be adjusted to match the value of R_1 but rather its value is adjusted to meet (5). This adjustment is necessary for calibration any way, and can be carried out as follows.